Chronological Changes in the Ultrastructure of Titanium-Bone Interfaces: Analysis by Light Microscopy, Transmission Electron Microscopy, and Micro-Computed Tomography

Kenzo Morinaga, DDS;* Hirofumi Kido, DDS, PhD;† Atsuko Sato, PhD;‡ Akira Watazu, PhD;§ Masaro Matsuura, DDS, PhD¶

ABSTRACT

Purposes: The objectives of this study were to chronologically examine the titanium-bone interfaces and to clarify the process of osseointegration using light microscopy, transmission electron microscopy (TEM), and micro-computed tomography (CT).

Materials and Methods: Experimental implants (Ti-coating plastic implants) were placed into tibiae of 8-week-old rats. Animals were sacrificed at 1 to 28 days after implant placement and prepared tissue specimens for a light microscope, a TEM, and micro-CT.

Results: New bone formation began 5 days after implant placement, and osseointegration was obtained by 14 days after implant placement. Osseointegration was well developed by 28 days after implant placement.

Discussion: TEM and quantitative computer tomography (QCT) results indicated that bone formation in osseointegration of titanium implants did not occur from the surfaces of the implant or preexisting bone, but it was likely that bone formation progressed at a site a small distance away from the surface. The bone formation took place in a scattered manner. Small bone fragments adhered to each other and transformed into reticular-shaped bone, and finally these bones became lamellar bone.

Conclusion: Comparative analysis of the titanium-bone interfaces using light microscopy, TEM, and QCT by micro-CT revealed the precise process of osseointegration.

KEY WORDS: chronological observation, micro-CT, osseointegration, quantitative computer tomography, titanium coating, ultrastructure

Osseointegration is an important factor in determining the outcome of titanium implants. The analysis of its mechanism is an important research topic in implant performance evaluation and improving the outcome of implants.

For the histological evaluation of implants, many reports have described the preparation of ground specimens and methods of comparing the contact rates between the implant surface and bone.[1–3] Studies have been conducted using electron microscopy for more detailed observations.[1–25] Because the implants were

*Graduate student, section of oral implantology, Department of Oral Rehabilitation, Fukuoka Dental College, 2-15-1 Tamura, Sawara-ku, Fukuoka, 814-0193, Japan; †associate professor, section of oral implantology, Department of Oral Rehabilitation, Fukuoka Dental College, 2-15-1 Tamura, Sawara-ku, Fukuoka, 814-0193, Japan; ‡professor, section of functional structure, Department of Morphological Biology, Fukuoka Dental College, 2-15-1 Tamura, Sawara-ku, Fukuoka, 814-0193, Japan; §research scientist, National Institute of Advance Industrial Science and Technology (AIST), 2266-98 Anagahora, Shimoshidami, Moriyama-ku, Nagoya 463-8560, Japan; ¶professor, section of oral implantology, Department of Oral Rehabilitation, Fukuoka Dental College, 2-15-1 Tamura, Sawara-ku, Fukuoka, 814-0193, Japan

Reprint requests: Dr. Hirofumi Kido, Section of Oral Implantology, Department of Oral Rehabilitation, Fukuoka Dental College, 2-15-1 Tamura, Sawara-ku, Fukuoka, 814-0193, Japan; e-mail: hkido@college.fdcnet.ac.jp

DOI 10.1111/j.1708-8208.2008.00093.x

metallic, it was technically difficult to prepare specimens which allowed the examination of an intact titanium-bone interface.[4–16] Another reported method is the analysis of peri-implant tissues by micro-computed tomography (CT).[26–31] The utility of micro-CT is gaining interest. This method allows for accurate measurements. In addition, bone mineral density (BMD) can be measured by quantitative computer tomography (QCT), and it can be applied to a finite element method.[26–28] However, artifacts develop around the implant bodies because the implants are radiopaque. Accurate observations of the implant-bone interfaces have been difficult.[29–31] Therefore, we fabricated titanium-coated plastic implants from which sections for transmission electron microscopy (TEM) could be prepared.[17] This study was conducted to improve these experimental implants so that they are more compatible with light microscopy, TEM, and micro-CT. These implants were placed in rat tibiae and were chronologically examined. The objective of this study was to clarify the process of osseointegration using this system.

MATERIALS AND METHODS

Experimental Implants

The experimental implants were fabricated following the method of Okamatsu and colleagues,[17] namely, a thin film of titanium was coated on the axial surface of a plastic rod with 1.6 mm diameter and 7 mm length. A DC sputtering apparatus (L332S-FHS, ANELVA, Tokyo, Japan) was used for titanium coating.[32,33] Sputtering was performed with a target using titanium of 99.9% purity and under a 2.2×10^{-1} Pa argon atmosphere. It is better to make the titanium film thin to facilitate the examination of titanium-bone interface. Therefore, we adjusted the sputtering time using the method of Okamatsu and colleagues[17] so that the film would be thin. Plastic implants without coatings were used as controls.

Surgical Procedure

Placements of implants were performed following the method of Okamatsu and colleagues.[17] The experimental animals were male Sprague Dawley rats which were 8 weeks old. Forty rats were used in this study. An implant socket was placed 10 mm inferiorly from the apical region of the knee joint, and the socket was prepared by a drill so that it penetrated from the tibial lateral to the medial side with 1.6 mm in diameter. One implant, an experimental or control implant, was placed in the prepared implant socket in either the left or right tibia. After the placement of implants, the periosteal flaps were sutured into appropriate positions, and the surgical treatment was then completed. This study was carried out under the control of the Animal Experimentation Committee at Fukuoka Dental College (approval number 03005).

Preparation of Samples for Light and Electron Microscopy

Perfusion fixation was performed under intravenous anesthesia at 1, 3, 5, 7, 14, and 28 days after implant placement. The preparation of samples was performed following the methods of previous study.[17]

The observed region was in the medial posterior area of the tibia to avoid the effects of stress caused by muscular activities. Observations were made at the area where the experimental implant penetrated the cortical bone (CB) and where it penetrated the bone marrow (BM).

Preparation of Samples for Micro-CT

Experimental implants were placed into rat tibiae using the same method as described. The rats were sacrificed at 3, 5, 7, 9, 11, 13, 14, and 28 days after implant placement. The tissues surrounding the experimental implants were collected for micro-CT imaging. The collected samples were imaged using micro-CT (Scan Xmate: E090S, Comscan Techno, Kanagawa, Japan). The imaging was performed using a cone beam scan, and the conditions were: 30 kV tube voltage, 250 μA tube current, and 7 μm slice thickness. Six hundred slices were required for imaging the entire experimental implant. For BMD measurements by QCT, a phantom for bone mineral measurements was imaged with the samples. A phantom designed for micro-CT was composed of seven types of hydroxyapatites (HAs) of known densities. The resin densities range from 200 to 800 mg/cm^3 and in 100 mg/cm^3 increments. An aluminum rod with 2,690 mg/cm^3 weight density was used as a BMD phantom. A calibration curve which converted the CT intensities (CT values) to BMD values was prepared.

The CT data were transmitted to a workstation, and three-dimensional reconstruction was performed using software for three-dimensional trabecular structure measurements (TRI/3D-BON, Ratoc System Engineering Co. Ltd., Tokyo, Japan). In the axial cross-sections of the imaged experimental implants, the CT intensity of

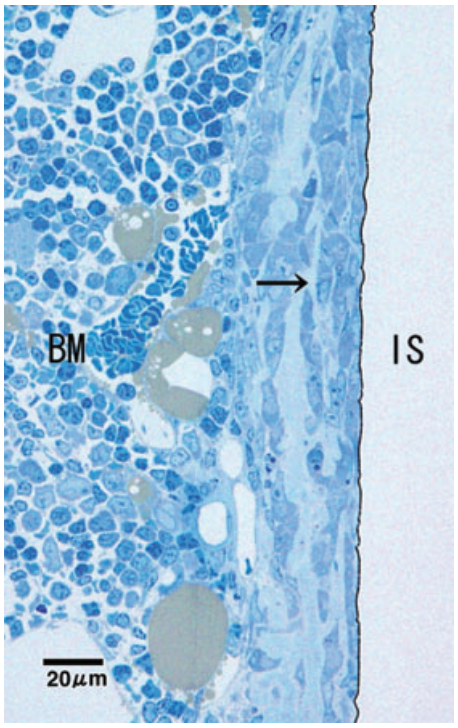

Figure 1 Light microscope image on the side of the bone marrow (BM) 5 days after implant placement. An alignment of flat cells on the side of the titanium surface is observed (arrow). IS, implant space.

each pixel was converted into BMD (mg/cm^3) using the calibration curve and displayed by different colors according to density.

RESULTS

All experimental animals recovered well after implant placement without any complications. Their conditions were well maintained until they were sacrificed. No inflammation was observed at the time of sacrifice.

Light microscope images at day 5 after the implant placement produced similar findings to those of day 3. Namely, the flat cells were observed aligned on the implant surface and on the side of the BM, a few dozen microns away from the implant surface (Figure 1). In the CB area, there were flat cells on the surfaces of the titanium and preexisting bone (Figure 2).

In the electron microscope images, flat osteoblasts (OBs) with developed granular endoplasmic reticula were observed along the surfaces of the implant and preexisting bone (Figure 3, A and B). The images show, on the surfaces of the preexisting bone and titanium, OBs secreting collagen fibers and the beginning of calcification with collagen fibers being used as a scaffold (Figure 4). OBs were observed in some regions away from the implant surface.

In the micro-CT images, calcified tissues thought to be a small amount of new bone were observed in some areas along the implant surroundings between the implant surface and the preexisting trabecular bone. The BMD values of the new bone were low ranging from 0 to 300 mg/cm^3 (blue). The BMD of the CB at the implant penetrated region (999 to 1,332 mg/cm^3) showed higher values than other CB areas (333 to 666 mg/cm^3) (Figure 5).

Micro-CT images at day 9 after the implant placement showed some new bones that were formed in some areas adhered to each other, and these bones transformed into reticular bone and surrounded the implant surface. There was an increase in the BMD values in the region of 600 to 1,200 mg/cm^3 (yellow green to yellow) (Figure 6).

In the micro-CT images at day 13 after the implant placement, the new bone of reticular shape was increased and most areas of the peri-implant new bone had BMD values of 600 to 1,200 mg/cm^3 (yellow green to yellow). At this time period, most BMD values were in the region of 0 to 1,000 mg/cm^3 (blue to yellow green) in the region from the peri-implant area to approximately 500 μm from that area (Figure 7).

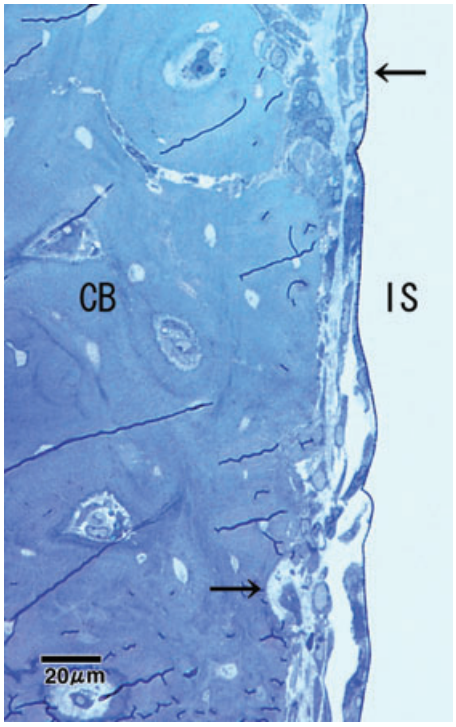

Figure 2 Light microscope image on the side of the cortical bone (CB) 5 days after implant placement. On the side of the CB, flat cells between the surfaces of the titanium and preexisting bone are observed (arrows). IS, implant space.

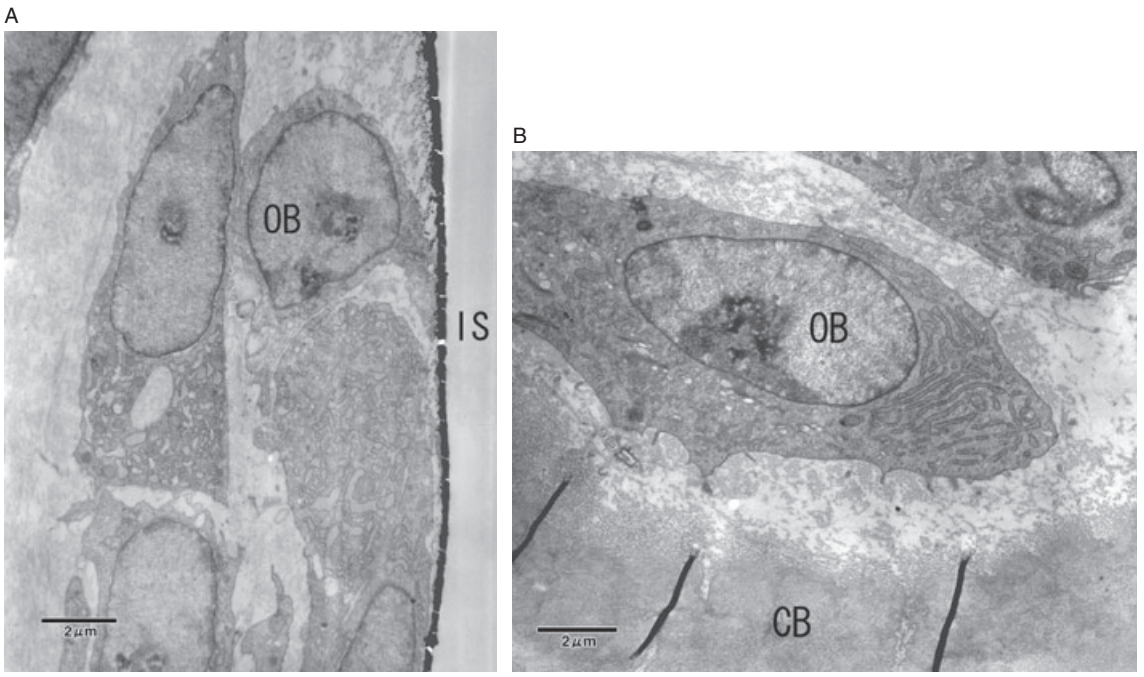

Figure 3 Electron microscope images on the side of the cortical bone (CB) 5 days after implant placement. Flat osteoblasts (OB) with developed granular endoplasmic reticula are observed along the surfaces of the titanium (IS) (A) and CB (B).

Light microscope images at day 14 after the implant placement showed that the new bone had directly contacted the implant. The new bone became layered and covered the titanium surface (Figure 8).

Electron microscope images indicated a collagen layer that had coursed parallel to the implant surface. The so-called "amorphous layer" was not observed at the implant-bone interface (Figure 9).

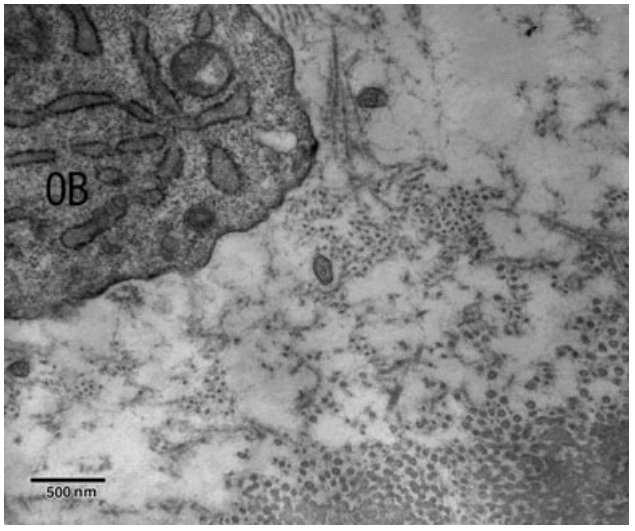

Figure 4 Electron microscope image 5 days after implant placement. Collagen fibers are observed around osteoblasts (OB).

The micro-CT images showed the part of the reticular bone which had transformed into lamellar bone. The amount of calcification tended to decrease in the region away from the implant surface. (Figure 10).

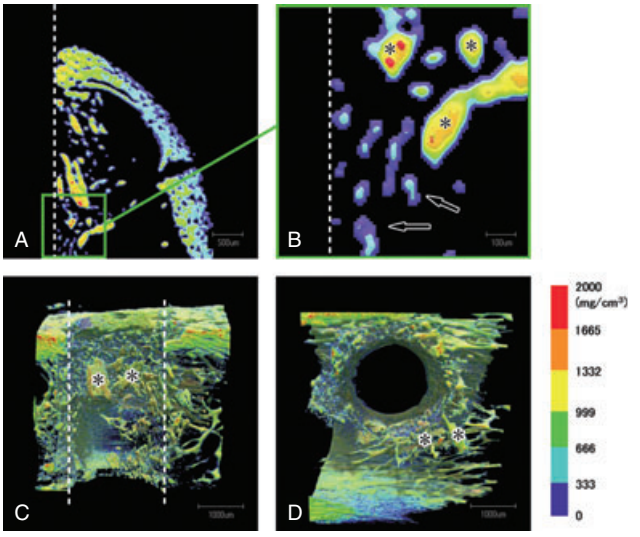

Figure 5 Bone mineral density (BMD) longitudinal section (A–C) and three-dimensional image (C, D) 5 days after the implant placement. (A) Longitudinal section of implant with BMD (low magnification). The BMD of the cortical bone (CB) at the implant penetrated region (999 to 1,332 mg/cm^3) shows higher values than other CB areas (333 to 666 mg/cm^3). (B) Bone marrow region (high magnification). Calcified tissue thought to be a small amount of new bone along the implant (arrows). (C) Longitudinal section. (D) Cross section. The outline of the implant (white dotted line), debris of preexisting bone (*).

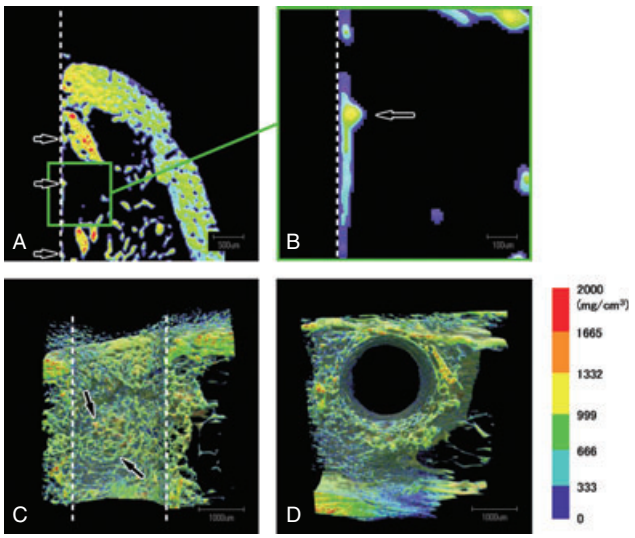

Figure 6 Bone mineral density (BMD) longitudinal section (A–C) and three-dimensional image (C, D) 9 days after the implant placement. (A) Some mineralized tissues are observed (arrows). (B) The higher BMD is observed in the center of the mineralized tissue along the implant surface (arrow). (C) Some new bones that are formed in some areas adhere to each other, and these bones have transformed into trabecular bone and surrounded the implant surface (arrows). (D) A lot of trabecular bone surrounding implant. The outline of the implant (white dotted line).

Light microscope images at day 28 after the implant placement showed that peri-implant new bone covered the implant body continuously. The so-called "osseointegration" was achieved (Figure 11).

The thickness of the new bone on the titanium surface was increased in the electron microscope images. The osteocytes had protrusions extending toward the titanium surface. On the titanium surface, a layer of approximately 200 nm thickness with indistinct structure was observed with high electron density and another layer with low electron density. These layers were not necessarily seen around the entire circumference of titanium (Figure 12).

The micro-CT images showed that most of the reticular bone adhered to each other and transformed into lamellar bone. The BMD values of the new bone were 900 to 1,300 mg/cm^3 (yellow to red). The density was similar to the preexisting bone. Calcified tissue, which was seen away from the implant surface on or before day 13, had mostly disappeared. Bone tissue densely covering the implant surface was seen. The BMD of the CB at the implant penetrated region (1,665 to 2,000 mg/cm^3) showed higher values than other CB areas (1,332 to 1,665 mg/cm^3) (Figure 13).

DISCUSSION

The analysis of the union between titanium and bone is very important in the evaluation of titanium implants. Because it is technically difficult, there are only a few reports on the ultrastructure of the intact bone-titanium interface and its surrounding tissue. In the preparation of samples for observation, the following have been attempted: implant fracture technique to remove the implants[4–16] and a technique using plastic implants coated with titanium foil.[17–25] There is a risk of damaging the titanium-bone interface in the former technique because an implant is removed. An intact interface can be observed by the technique involving the titanium-coated plastic implant. This experimental method is considered to be a superior technique. However, the number of reports using this technique is even smaller, and there are variabilities in the properties of thin titanium film among reports.[17–25] Okamatsu and colleagues[17] coated titanium using the DC magnetron sputtering method. They were able to attain an even titanium coating of 150 to 250 nm, and they confirmed osseointegration by light and electron microscopy. In this study, we minimized tissue damage during the

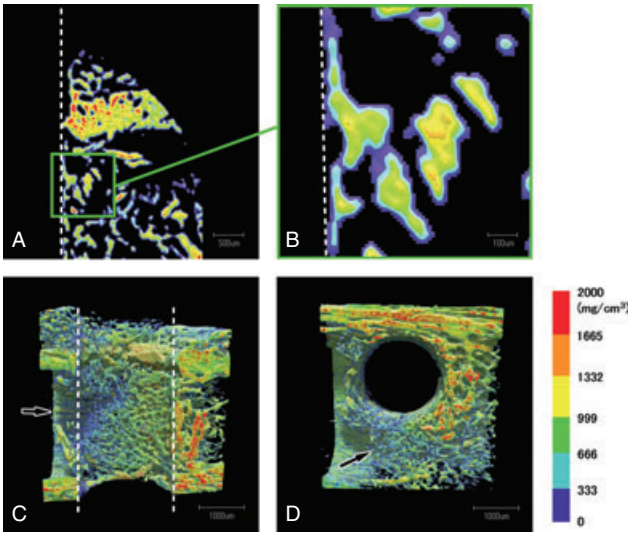

Figure 7 Bone mineral density (BMD) longitudinal section (A–C) and three-dimensional image (C, D) 13 days after the implant placement. (A) The BMD of the cortical bone (CB) at the implant penetrated region (1,665 to 2,000 mg/cm^3) shows higher values than other CB areas (999 to 1,332 mg/cm^3). (B) The BMD of the new bone is increased (999 to 1,332 mg/cm^3). (C, D) The trabecular bone is increased. BMD values of most areas of the peri-implant new bone are 600 to 1,200 mg/cm^3 (yellow green to yellow). Most of the BMD values are 0 to 1,000 mg/cm^3 (blue to yellow green) from the peri-implant area to approximately 500 μm away from it (arrows). The outline of the implant (white dotted line).

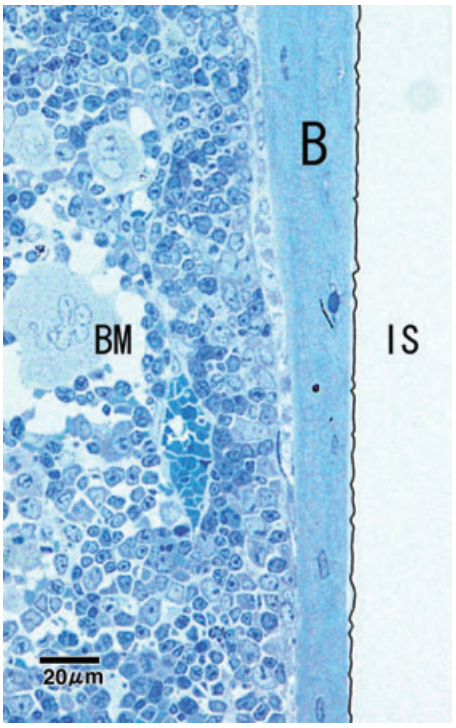

Figure 8 Light microscope image on the side of the bone marrow (BM) 14 days after implant placement. New bone (B) is layered. It is directly contacting the implant and covering the titanium surface (IS).

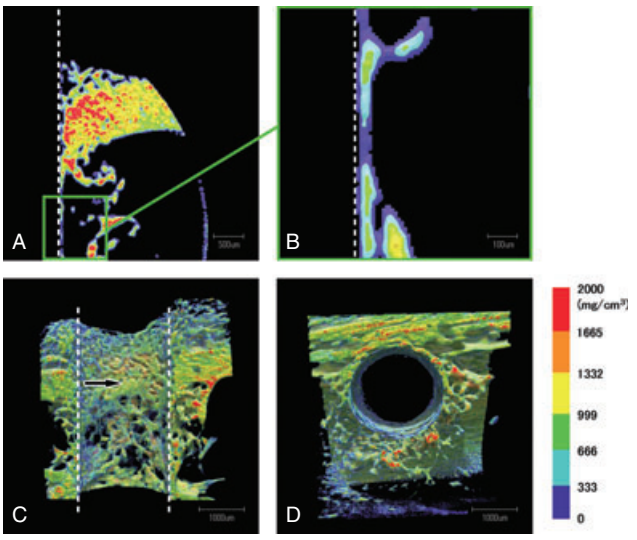

Figure 10 Bone mineral density (BMD) longitudinal section (A–C) and three-dimensional image (C, D) 14 days after the implant placement. (A) The BMD of the cortical bone (CB) at the implant penetrated region (1,665 to 2,000 mg/cm^3) shows higher values than other CB areas (1,332 to 1,665 mg/cm^3). (C, D) A part of the trabecular bone has transformed into lamellar bone (arrow). Lamellar new bone covers the implant circumferentially, but the amount of calcification in the area away from the implant surface tends to be reduced.

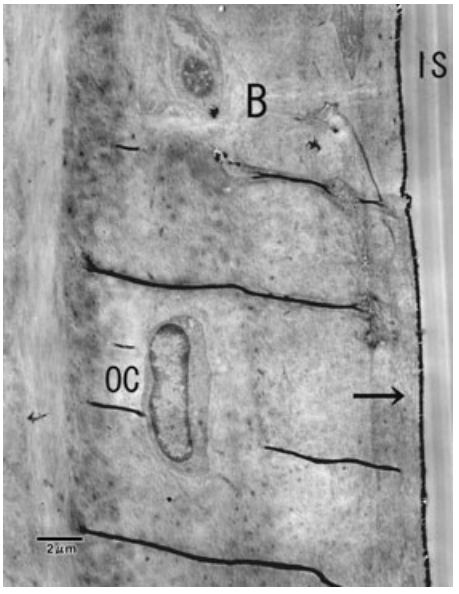

Figure 9 Electron microscope image on the side of the bone marrow (BM) 14 days after implant placement. A collagen layer that has coursed parallel to the implant surface (IS) is observed. The so-called "amorphous layer" at the implant-bone interface is not observed (arrow). OC, osteocyte.

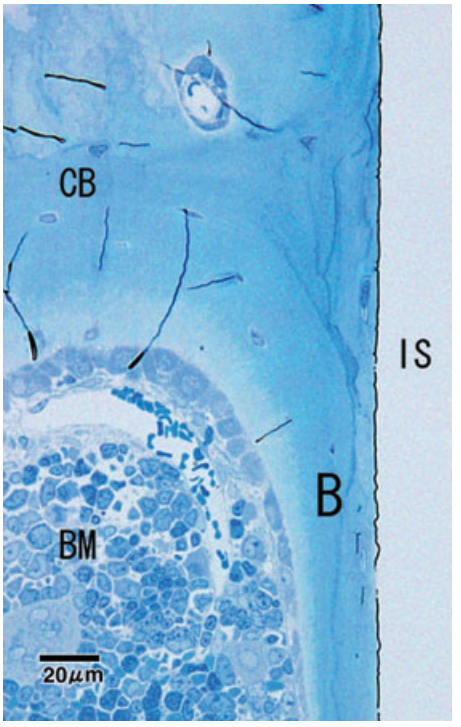

Figure 11 Light microscope image 28 days after implant placement. Peri-implant new bone (B) continuously covers the implant body (IS). The so-called "osseointegration" is attained.

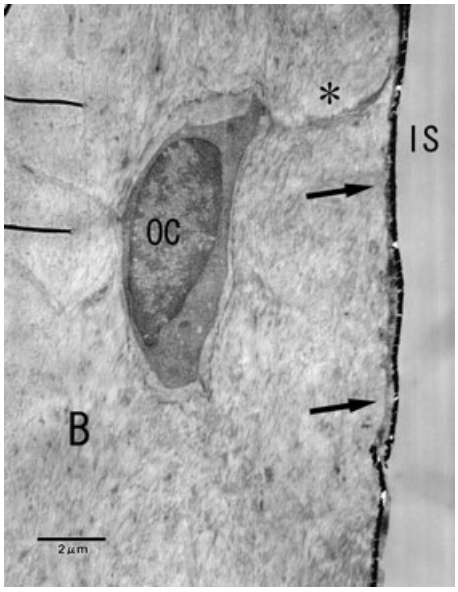

Figure 12 Electron microscope image 28 days after implant placement. Protrusions (*) extend from the osteocyte (OC) incorporate into the bone to the titanium surface (IS). On the titanium surface, a layer of approximately 200 nm thickness with indistinct structure is observed with high electron density and another layer with low electron density (arrows).

preparation of specimens, and minimize the effect of metal artifacts in the examination by micro-CT. To achieve these goals, we created a thinner titanium coating layer by approximately halving the sputtering time.

In 1982, Albrektsson and colleagues[19] coated a titanium film of 2,000 Å onto polycarbonate implants and examined them under the electron microscope. They reported that the course of collagen fibers in the bone adjacent to the titanium surface was in a mesh form. Thereafter, several reports were made on titanium-coated plastic implants.[17–25] However, their observation periods and properties of the coating were varied. Therefore, consensus has not been reached on the structure of the titanium-bone interface. Although reports have examined tissues surrounding plastic implants coated with titanium, none analyzed the process from implant placement until osseointegration.

There have been reports on studies using the fracture technique on the maxillae of rats and performing chronological observations. Futami and colleagues[9] placed titanium implants with machined surfaces in rats' maxillae. They collected samples at 1, 3, 5, 7, 14, and 28 days later and examined them using TEM. As a result, bone formation began 5 days after the implant placement. The bone formation started from the side of the preexisting bone of the implant socket. They also found that bone formation was different between the lateral and base portions of the implant. They stated that the difference was dependent on the size of the gap between the implant and the preexisting bone. In a study by the same research group, Shirakura and colleagues[10] performed an analysis similar to Futami and colleagues[9] in sandblasted titanium implants and HA-coated implants. In both types of implants, bone formation began 5 days after the implant placement. Bone formation began from the preexisting bone in the sandblasted implants, while it began from the implant surface in the HA-coated implants.

In our study, we found that bone formation began 5 days after the implant placement, as in past studies. As in the report of Futami and colleagues,[9] we observed cells which were adhered to the implant surface. We did not observe bone formation from the implant surface. The marrow areas of the rat tibiae had practically no trabecular bone, and the majority of the implant surfaces were adjacent to the BM tissue at implant placement. In the micro-CT, tissue with high BMD was observed in the area away from the implant surface. Bone formation was speculated to have begun a short distance away from the implant surface (30 to 50 μm).

Micro-CT is a highly useful method for measuring detailed morphology of the bone. Micro-CT data allow

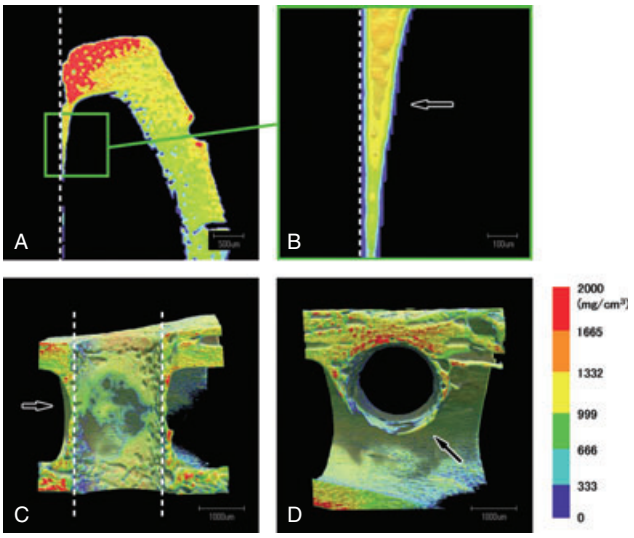

Figure 13 Bone mineral density (BMD) longitudinal section (A–C) and three-dimensional image (C, D) 28 days after the implant placement. (A) The BMD of the cortical bone (CB) at the implant penetrated region (1,665 to 2,000 mg/cm^3) shows higher values than other CB areas (1,332 to 1,665 mg/cm^3). (B) Formation of thick new bone is confirmed (arrow). BMD values of new bone are 900 to 1,300 mg/cm^3 (yellow to red). The density was similar to preexisting bone. (C, D) Only lamellar new bone surrounds implant (arrows).

for any cross section and three-dimensional image reconstruction. In addition, the data can be used in a finite element method and other methods using computer simulation. Therefore, there are many reports in which micro-CT was used to examine the calcified tissues surrounding the implants.[26–31] These reports used metallic implants. Therefore, artifacts around the implants occurred, and observation of areas adjacent to the implants was reported to be difficult. Oosterwyck and colleagues[29] placed implants each with 4 mm diameter and 12 mm length in the femoral condyles of sheep. They compared the results of observation using micro-CT and from tissue specimens. As a result, trabecular bone structure in both methods was very similar. They reported that data can be used in a finite element method. In addition, they stated that there were no significant artifacts, but artifacts occurred at the apex of the thread of the implant. Butz and colleagues[30] placed titanium implants in rat femurs and morphologically compared the micro-CT images and tissue specimens. As a result, because of the effects of the metal artifacts, there was a significant difference between the two methods from the implant surface to 24 μm away from it. Stoppie and colleagues[31] also performed a similar study using titanium implants in the femurs of sheep. They reported that there were effects of metal artifacts in an area 60 μm surrounding the implants.

In our study, we used a phantom developed exclusively for micro-CT, and we measured BMD (mg/cm^3) using QCT. When three-dimensional images from QCT were examined chronologically, we obtained interesting findings. Five to nine days after the implant placement, formation of tissues with low BMD (<300 mg/cm^3) was extensively found from the implant surface to a few hundred microns from it. However, not all of these calcified tissues became mature bone. By 14 days after the implant placement, parts of these tissues transformed into reticular bone. Furthermore, it was replaced by plate-shaped tissues with high density (300 to 1,000 mg/cm^3) that were observed on the implant surface. In TEM from this time period, bone formation was observed contacting the titanium surface. The course of collagen in the bone and the thickness of the fibers were different from the mature preexisting bone. Also, in this time period, the so-called "amorphous layer" was mostly not observed. The amorphous layer was observed frequently in TEM 28 days after the implant placement. As Okamatsu and colleagues[17] speculated, formation of the amorphous layer was thought to be related to the maturation of the peri-implant bone and the progression of osseointegration.

The results of QCT 28 days after implant placement showed that plate-shaped new bone formed in the peri-implant tissue had high BMD in the middle and low BMD in the surroundings. The past studies reported that bone formation occurred from the entire implant surface toward the BM. We, however, revealed that the bone formation took place in a scattered manner. Small bone fragments adhered to each other and transformed into trabecular bone, and finally these bones became lamellar bone. In this process, the bone formation occurred extensively in the region away from the titanium surface. It was a temporary phenomenon that disappeared after the osseointegration was achieved. These findings indicate that in the process of osseointegration of titanium implants, bone formation does not begin at the surfaces of the implant or preexisting bone, but that calcification progresses at a site a small distance away from the surface. The BMD of the CB was increased with time. In particular, the BMD of the CB at the implant penetrated region was higher than the other regions.

CONCLUSION

In the period 5 to 9 days after implant placement, formation of calcified tissue with low BMD was seen extensively in the area 500 μm away from the implant surface. The calcified tissue disappeared by 14 days after the implant placement. Lamellar bone with high density was observed contacting the implant surface 28 days after implant placement.

TEM and QCT results indicated that bone formation in osseointegration of titanium implants did not occur from the surfaces of the implant or preexisting bone, but it was likely that bone formation progressed at a site a small distance away from the surface. The bone formation took place in a scattered manner. Small bone fragments adhered to each other and transformed into trabecular bone, and finally these bones became lamellar bone.

We rarely observed an amorphous layer in the specimens 14 days after implant placement, but it was frequently observed in the specimens 28 days after the implant placement. These findings suggested that formation of amorphous layer was related to the maturation of the peri-implant bone and the progression of osseointegration.

New bone formation in rats began 5 days after implant placement, and osseointegration was obtained by 14 days after implant placement. Osseointegration was well developed by 28 days after implant placement.

We adjusted the thickness of the coating by reducing the sputtering time in the preparation of the titanium-coated implants. As a result, we reduced damage to tissues in the preparation of specimens and we were able to observe clearly the tissue ultrastructure adjacent to the titanium.

Metal artifacts were not seen in the micro-CT of titanium-coated implants prepared in our study. Therefore, this type of implant is useful in observing the microstructure of calcified tissue at the titanium-bone interface and in measuring BMD values.

ACKNOWLEDGMENT

The authors would like to thank Dr. Toshikazu Nagato, prof. ret. of Fukuoka Dental College, and Prof. Hironobu Sato, Section of Fixed Prosthodontics, Department of Oral Rehabilitation, for valuable advice. We also wish to thank Dr. Kae Okamatsu, section of oral implantology, Department of Oral Rehabilitation, Fukuoka Dental College, and Mr. Koichiro Morishita, Department of Morphological Biology, Fukuoka Dental College, for assistance in operating the electron microscope. This work was partly supported by a Grant-in-Aid 19592276 from the Ministry of Education, Culture Sports, Science and Technology, Japan.

REFERENCES

1. Albrektsson TO, Johansson C, Sennerby L. Biological aspects of implant dentistry: osseointegration. Periodontol 2000 1994; 4:58–73.
2. Brånemark PI. Osseointegration: biotechnological perspective and clinical modality. In: Brånemark PI, Rydevik BL, Skalak R, eds. Osseointegration in skeletal reconstruction and joint replacement. Chicago, IL: Quintessence, 1997:1–24.
3. Albrektsson T, Brånemark PI, Hansson HA, Lindström J. Osseointegrated titanium implants. Requirements for ensuring a long-lasting, direct bone-to-implant anchorage in man. Acta Orthop Scand 1981; 52:155–170.
4. Steflik DE, Sisk AL, Perr GA, Lake FT, Hanes PJ. Experimental studies of the implant-tissue interface. J Oral Implantol 1993; 19:90–94.
5. Steflik DE, Corpe RS, Lake FT, et al. Ultrastructural analyses of the attachment (bonding) zone between bone and implanted biomaterials. J Biomed Mater Res 1998; 39:611–620.
6. Steflik DE, Parr GR, Sisk AL, et al. Osteoblast activity at the dental implant-bone interface: transmission electron microscopic and high voltage electron microscopic observations. J Periodontol 1994; 65:404–413.
7. Asawa Y, Aoki K, Ohya K, Oshima H, Takano Y. Appearance of electron-dense segments: indication of possible conformational changes of pre-mineralizing collagen fibrils in the osteoid of rat bones. J Electron Microsc (Tokyo) 2004; 53:426–433.
8. Puleo DA, Nanci A. Understanding and controlling the bone-implant interface. Biomaterials 1999; 20:2311–2321.
9. Futami T, Fujii N, Ohnishi H, et al. Tissue response to titanium implants in the rat maxilla: ultrastructural and histochemical observations of the bone-titanium interface. J Periodontol 2000; 71:287–298.
10. Shirakura M, Fujii N, Ohnishi H, et al. Tissue response to titanium implantation in the rat maxilla, with special reference to the effects of surface conditions on bone formation. Clin Oral Implants Res 2003; 14:687–696.
11. Masuda T, Salvi GE, Offenbacher S, Felton DA, Cooper LF. Cell and matrix reactions at titanium implants in surgically prepared rat tibiae. Int J Oral Maxillofac Implants 1997; 12:472–485.
12. Sennerby L, Thomsen P, Ericson LE. Early tissue response to titanium implants inserted in rabbit cortical bone. Part II: ultrastructural observations. J Mater Sci Mater Med 1993; 4:494–502.
13. Nanci A, McCarthy GF, Zalzal S, Clokie CML, Warshawsky H, McKee MD. Tissue response to titanium implants in the rat tibia: ultrastructural, immunocytochemical and lectin-cytochemical characterization of the bone-titanium interface. Cell Mater 1994; 4:1–30.
14. Murai K, Takeshita F, Ayukawa Y, Kiyoshima T, Suetsugu T, Tanaka T. Light and microscopic studies of bone-titanium interface in the tibiae of young and mature rats. J Biomed Mater Res 1996; 30:523–533.
15. Ayukawa Y, Takeshita F, Inoue T, et al. An immunoelectron microscopic localization of noncollagenous bone proteins (osteocalcin and osteopontin) at the bone-titanium interface of rat tibiae. J Biomed Mater Res 1998; 41:111–119.
16. Chistophe M, Christian R, Christian C. A histological investigation on early tissue response to titanium implants in a rat intramedullary model. J Oral Implantol 2000; 26:238–243.
17. Okamatsu K, Kido H, Sato A, Watazu A, Matsuura M. Ultrastructure of the interface between titanium and surrounding tissue in rat tibiae – a comparison study on titanium-coated and -uncoated plastic implants. Clin Implant Dent Relat Res 2007; 9:100–111.
18. Albrektsson T, Jacobsson M. Bone-metal interface in osseointegration. J Prosthet Dent 1987; 57:597–607.
19. Albrektsson T, Brånemark PI, Hansson HA, Ivarsson B, Jönsson U. Ultrastructural analysis of the interface zone of

titanium and gold implants. Clin Appl Biomater 1982; 4:167–177.
20. Linder L, Albrektsson T, Brånemark PI, et al. Electron microscopic analysis of the bone-titanium interface. Acta Orthop Scand 1983; 54:45–52.
21. Albrektsson T, Hansson HA. An ultrastructural characterization of the interface between bone and sputtered titanium or stainless surfaces. Biomaterials 1986; 7:201–205.
22. Listgarten MA, Buser D, Steinemann SG, Donath K, Lang NP, Weber HP. Light and transmission electron microscopy of the intact interfaces between non-submerged titanium-coated epoxy resin implants and bone or gingiva. J Dent Res 1992; 71:364–371.
23. Ayukawa Y, Takeshita F, Inoue T, et al. An ultrastructural study of the bone-titanium interface using pure titanium-coated plastic and pure titanium root implants. Acta Histochem Cytochem 1996; 29:243–254.
24. Ayukawa Y, Takeshita F, Yoshinari M, et al. An immunocytochemical study for lysosomal cathepsins B and D related to the intracellular degradation of titanium at the bone-titanium interface. J Periodontol 1998; 69:62–68.
25. Chehroudi B, Gould TRL, Brunette DM. A light and electron microscopic study of the effects of surface topography on the behavior of cells attached to titanium-coated percutaneous implants. J Biomed Mater Res 1991; 25:387–405.
26. Joo YI, Sone T, Fukunaga M, Lim SG, Onodera S. Effects of endurance exercise on three-dimensional trabecular bone microarchitecture in young growing rats. Bone 2003; 33: 485–493.
27. Sone T, Tamada T, Jo Y, Miyoshi H, Fukunaga M. Analysis of three-dimensional microarchitecture and degree of mineralization in bone metastases from prostate cancer using synchrotron microcomputed tomography. Bone 2004; 35:432–438.
28. Ito M, Ikeda K, Nishiguchi M, et al. Multi-detector row CT imaging of vertebral microstructure for evaluation of fracture risk. J Bone Miner Res 2005; 20:1828–1836.
29. Oosterwyck HV, Duyck J, Sloten JV, et al. The use of microfocus computerized tomography as a new technique for characterizing bone tissue around oral implants. J Oral Implantol 2000; 26:5–12.
30. Butz F, Ogawa T, Chang TL, Nishimura I. Three-dimensional bone-implant integration profiling using micro-computed tomography. Int J Oral Maxillofac Implants 2006; 21:687–695.
31. Stoppie N, Waerden JP, Jansen JA, Duyck J, Wevers M, Naert IE. Validation of microfocus computed tomography in the evaluation of bone implant specimens. Clin Implant Dent Relat Res 2005; 7:87–94.
32. Watazu A, Teraoka K, Kido H, et al. An inverted observation technique for interactions between titanium oxide and cells on commercially pure titanium. Key Eng Mater 2006; 309–311:363–366.
33. Watazu A, Teraoka K, Kido H, et al. Formation and properties of transparent titanium thin films by DC magnetron sputtering for observing interactions between titanium and cells. Trans Mater Res Soc Jpn 2006; 31:677–680.